

Contents lists available at ScienceDirect

Chemosphere

journal homepage: www.elsevier.com/locate/chemosphere

Carbon and nitrogen stable isotope fractionation during abiotic hydrolysis of pesticides

Jérémy Masbou, Guillaume Drouin, Sylvain Payraudeau, Gwenaël Imfeld*

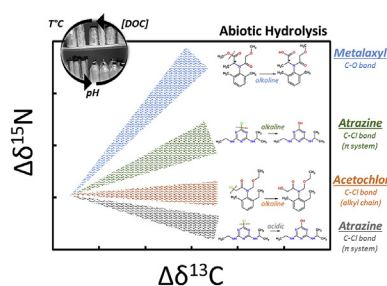
Laboratoire d'Hydrologie et de Géochimie de Strasbourg (LHyGeS), Université de Strasbourg/ENGEEES, CNRS, 1 rue Blessig, 67084, Strasbourg Cedex, France



HIGHLIGHTS

- C–N dual-CSIA and C-ESIA revealed isotopic fractionation during pesticide hydrolysis.
- Significant abiotic hydrolysis of the pesticides was observed at $\text{pH} \leq 4$ and ≥ 12 .
- No enantiomeric isotopic fractionation during abiotic hydrolysis of chiral Metalaxyl.
- Pathway-specific carbon and nitrogen isotopic fractionation are provided.

GRAPHICAL ABSTRACT



ARTICLE INFO

Article history:

Received 4 June 2018

Received in revised form

7 September 2018

Accepted 8 September 2018

Available online 10 September 2018

Handling Editor: Klaus Kümmerer

Keywords:

CSIA
ESIA
Hydrolysis
Pesticide degradation
Enantiomers

ABSTRACT

Compound-specific Stable Isotope Analysis (CSIA) has been recently established as a tool to study pesticide degradation in the environment. Among degradative processes, hydrolysis is environmentally relevant as it can be chemically or enzymatically mediated. Here, CSIA was used to examine stable carbon and nitrogen isotope fractionation during abiotic hydrolysis of legacy or currently used pesticides (chloroacetanilide herbicides: Acetochlor, Alachlor, S-Metolachlor and Butachlor, acylalanine fungicide: Metalaxyl, and triazine herbicide: Atrazine). Degradation products analysis and C–N dual-CSIA allowed to infer hydrolytic degradation pathways from carbon and nitrogen isotopic fractionation. Carbon isotopic fractionation for alkaline hydrolysis revealed similar apparent kinetic isotope effects ($\text{AKIE}_C = 1.03 - 1.07$) for the 6 pesticides, which were consistent with $\text{S}_{\text{N}}2$ type nucleophilic substitutions. Neither enantio-selectivity ($\text{EF} \approx 0.5$) nor enantio-specific isotope fractionation occurred during hydrolysis of R ($\text{AKIE}_C = 1.04 \pm 0.01$) and S ($\text{AKIE}_C = 1.04 \pm 0.02$) enantiomers of a racemic mixture of Metalaxyl. Dual element isotope plots enabled to tease apart C–Cl bond breaking of alkane ($\Delta \approx \epsilon_{\text{N}}/\epsilon_{\text{C}} \approx 0$, Acetochlor, Butachlor) and aromatic π -system ($\Delta \approx 0.2$, Atrazine) from C–O bond breaking by dealkylation ($\Delta \approx 0.9$, Metalaxyl). Reference values for abiotic versus biotic $\text{S}_{\text{N}}2$ reactions derived from carbon and nitrogen CSIA may be used to untangle pesticide degradation pathways and evaluate *in situ* degradation during natural and engineered remediation.

© 2018 Elsevier Ltd. All rights reserved.

1. Introduction

The frequent and ubiquitous detection of pesticides in ground- and surface-waters reflects their extensive use and persistence (Fenner et al., 2013). In the environment, pesticide concentrations mainly decrease by degradation, but also by non-degradative

* Corresponding author. Laboratoire d'Hydrologie et de Géochimie de Strasbourg (LHyGeS), Université de Strasbourg/ENGEEES, CNRS, 1 rue Blessig, 67084, Strasbourg Cedex, France.

E-mail address: imfeld@unistra.fr (G. Imfeld).

processes, such as dilution or sorption. This hinders the estimation of degradation extent in the field without detection of transformation products, which are often unknown, or establishment of mass balances. Hydrolysis is a major pathway of pesticide degradation, which can be abiotically or biologically-mediated (Mandelbaum et al., 1993; Meyer et al., 2009; Fenner et al., 2013), depending on pH, temperature (Mabey and Mill, 1978) or dissolved organic matter (Larson and Weber, 1994). However, degradation pathways, such as hydrolysis, first have to be related to specific transformation mechanisms to tease them apart in laboratory experiments, and to eventually evaluate dissipation pathways under field conditions.

In this context, Compound-specific Stable Isotope Analysis (CSIA) is useful to evaluate *in situ* pesticide degradation because it may provide independent estimates of pesticide degradation (Elsner, 2010; Elsner and Imfeld, 2016). Pesticide CSIA relies on the kinetic isotope effect (KIE) caused by slightly different cleavage rates of molecule's bonds containing light and heavy isotopes. In contrast, non-degradative processes, such as dilution, volatilization or sorption generally result in insignificant isotopic fractionation (Schüth et al., 2003; Wang and Huang, 2003; Imfeld et al., 2014; Zhang et al., 2014; Elsner and Imfeld, 2016). The isotopic fractionation ϵ relates changes of isotope ratios to the extent of degradation following a Rayleigh approach (Hoefs, 1997). Some reference ϵ values for specific biotic or abiotic transformation mechanisms of pesticides, were retrieved from laboratory experiments (Hartenbach et al., 2008; Meyer et al., 2009, 2014; Wu et al., 2017; Masbou et al., 2018). Changes in carbon isotope ratios are, however, smaller for larger molecules and may not be easily detected under field conditions because non-reactive positions 'dilute' isotope effects at the reacting bond (Elsner, 2010). In this case, dual element isotope plots of, e.g., $\epsilon_{\text{Nitrogen}}$ versus ϵ_{Carbon} , reveal the footprint of underlying isotope effects (Elsner and Imfeld, 2016). For example, N and C dual element isotope patterns enabled to discriminate bond cleavage mechanisms during abiotic (acidic and alkaline) and biotic hydrolysis of Atrazine in experimental (Meyer et al., 2008, 2009) and theoretical (Grzybkowska et al., 2014) studies. However, C and N isotope fractionation during hydrolysis of anilide pesticides have yet to be evaluated.

Among anilide pesticides, S-Metolachlor, Acetochlor and Alachlor are the most applied herbicides worldwide (Atwood and Paisley-Jones, 2017), Butachlor is commonly used in Indian rice fields (Armanpour and Bing, 2015), while Metalaxyl is a common fungicide in European vineyards (Komárek et al., 2010). Anilide pesticides are mainly made of carbon ($\approx 60\%$, Table 1) and change in $\delta^{13}\text{C}$ values have been used to evaluate chloroacetanilide degradation (Elsayed et al., 2014; Alvarez-Zaldívar et al., 2018). In

the case of chiral pesticides, such as Metalaxyl, CSIA and enantioselective analysis can be combined for Enantio-specific Stable Isotope Analysis (ESIA) to evaluate separately the isotope composition of each enantiomer (Badea and Danet, 2015; Masbou et al., 2018). Because substantial biodegradation can occur without significant deviations of the enantiomeric fractions (EFs), ESIA has become a promising new approach that can provide insight into enantioselective fates and source apportionment of environmental organic contaminants (Badea and Danet, 2015). Although high detection limits of isotope ratio mass spectrometry and small contribution of nitrogen (i.e., only one N heteroatom in the chloroacetanilides) challenge multi-element CSIA of anilide pesticides at environmental concentrations (Lutz et al., 2017), sample pre-concentration (>1000 times) recently allowed dual N and C-CSIA of S-Metolachlor at an agricultural catchment (Alvarez-Zaldívar et al., 2018). However, reference C and N isotopic fractionation ϵ for transformation reactions involving anilides are lacking so far. In addition, C–N isotope dual plots derived during hydrolysis may help to tease apart aqueous hydrolysis from other pathways of pesticide dissipation.

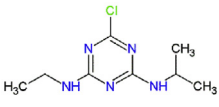
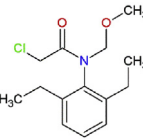
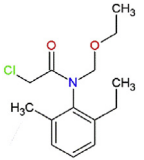
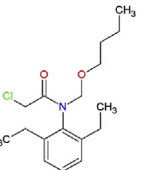
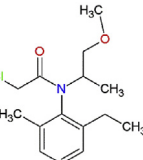
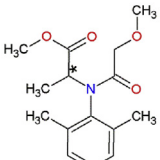
The objectives of this study were (i) to evaluate reaction kinetic rate constants for abiotic hydrolysis of chloroacetanilide herbicides (Alachlor, Acetochlor, S-Metolachlor, Butachlor), one chiral acylalanine fungicide (Metalaxyl), and one triazine herbicide (Atrazine) as a function of pH, T°C and dissolved organic carbon concentrations that may occur in natural water, (ii) to derive reference carbon (ϵ_{C}) and nitrogen (ϵ_{N}) isotopic fractionations during pesticide hydrolysis, (iii) to identify degradation mechanisms of pesticide degradation during abiotic hydrolysis using AKIE values and C–N dual isotope plots, and (iv) to evaluate enantioselective degradation of the chiral fungicide Metalaxyl during abiotic hydrolysis. Gas chromatography combustion isotope ratio mass spectrometry (GC–C-IRMS) methods were developed for $\delta^{13}\text{C}$ and $\delta^{15}\text{N}$ analysis of pesticides and used together with parent compounds and degradation products analysis to evaluate isotopic fractionation during abiotic hydrolysis as a function of pH (from 2 to 12), temperature (T°C, 20 °C and 30 °C) and dissolved organic carbon concentration (DOC, from 0 to 20 mg L⁻¹).

2. Materials and methods

2.1. Chemicals and solution preparation

Chloroacetanilides (Alachlor, Acetochlor, Butachlor, S-Metolachlor), Atrazine, racemic Metalaxyl (rac-Metalaxyl, 50% R and 50% S-Metalaxyl) and M-Metalaxyl (R enantiomer enriched Metalaxyl, 97%) standards (analytical grade purity: 99.6%), Metolachlor-d11

Table 1
Physico-chemical properties and chemical structures of studied pesticides.

	Triazine	Chloroacetanilide				Acylalanine
	Atrazine	Alachlor	Acetochlor	Butachlor	S-Metolachlor	Metalaxyl
Molecular formula	C ₈ H ₁₄ ClN ₅	C ₁₄ H ₂₀ ClNO ₂	C ₁₄ H ₂₀ ClNO ₂	C ₁₇ H ₂₆ ClNO ₂	C ₁₅ H ₂₂ ClNO ₂	C ₁₅ H ₂₁ NO ₄
Molecular structure						
Molar mass (g mol ⁻¹) ^a	215.7	269.8	269.8	311.8	283.8	279.3
Solubility in water (20–25 °C, mg L ⁻¹) ^a	35	240	282	20	530	8400
Dissociation constant (pKa) ^a	1.60	Non-Ionizable	Non-Ionizable	Non-Ionizable	Non-Ionizable	0

^a Data from (Lewis et al., 2016).

and Alachlor-d13 (analytical grade purity, > 97%), solvents (dichloromethane DCM, acetonitrile CAN, ethyl acetate EtOAc; HPLC grade purity, > 99.9%) were purchased from Sigma–Aldrich (St. Louis, MO, USA). Sodium hydroxide (BioUltra, ≥ 98.0%), potassium phthalate (≥ 99.5%), potassium chloride (BioReagent, ≥ 99.0%), potassium phosphate (≥ 99.0%), boric acid (BioReagent, ≥ 99.5%), calcium chloride dehydrate (≥ 99.0%) and humic acid sodium salt (technical grade) were purchased from Sigma–Aldrich (St. Louis, MO, USA).

Stock solutions for water spiking and standards for chromatographic analysis were prepared at 5 g L⁻¹ as individual pesticide or mix solutions in DCM and ACN, respectively. Aliquots of the solutions were stored at -20 °C until use and/or analysis. Physicochemical properties of the pesticides used in the experiment are listed in Table 1.

2.2. Abiotic hydrolysis experiment

Hydrolysis depends on pH and temperature (Mabey and Mill, 1978), but dissolved organic carbon in aquatic environment may also alter pesticide hydrolytic patterns (Larson and Weber, 1994). Duplicate abiotic hydrolysis experiments were carried out in 1 L Schott glass bottles under dark and sterile conditions (OECD, 2004). Five aqueous buffer solutions (1 L) were prepared at pH = 2, 4, 7, 9 and 12 (details in section S-1 of the SI), sterilized by filtration through a 0.22 μm cellulose membrane (Rotilabo[®], Carl Roth[®], France) and split in autoclaved Schott bottles. Experiments with dissolved organic carbon (DOC) were carried out at pH = 7 for approaching environmental conditions. Briefly, humic acid salts dissolved in 0.1 mol L⁻¹ NaOH solution by 45 min sonication (Mazzuoli et al., 2003) were filtered on 0.22 μm cellulose membranes (Rotilabo[®], Carl Roth[®], France) and adjusted to pH = 7 to reach final DOC concentrations of 4.9, 10.7 and 20.3 ± 0.1 mg C L⁻¹.

Buffer solutions were spiked with 3.2 mg L⁻¹ (≈ 12 μmol L⁻¹) of Alachlor, Acetochlor, Metalaxyl and S-Metolachlor, 4.3 mg L⁻¹ (≈ 20 μmol L⁻¹) for Atrazine and 2.4 mg L⁻¹ (≈ 8 μmol L⁻¹) for Butachlor from a 5 g L⁻¹ stock solution in DCM. The solutions were stirred at 20 °C until total DCM evaporation. Intermolecular effects between pesticides were negligible at those concentrations as confirmed by very similar results obtained for Atrazine in our study compared to previous studies with Atrazine only ((Meyer et al., 2008), see Part 3.2.). Bottles were tightly capped with screw caps (Schott), covered with aluminum foil and incubated separately at 20 ± 1 °C and 30 ± 1 °C. From 20 mL to 100 mL of different buffers were sampled at t = 0 (all conditions), t = 9 (all), t = 22 (pH = 12), t = 30 (pH = 12), t = 36 (all), t = 44 (pH = 12), t = 57 (pH = 12), t = 94 (all), t = 200 days (all), depending on pH conditions and dissipation kinetics.

2.3. Pesticide analysis

Solid phase extractions (SPE) of water samples were carried out using SolEx C18 cartridges (1 g, Dionex[®], CA, USA) and an AutoTrace 280 SPE system (Dionex[®], CA, USA) (Elsayed et al., 2014). Briefly, extraction cartridges were washed with 5 mL ethanol, rinsed with ACN (5 mL), conditioned with deionized water (10 mL), loaded with samples and dried under nitrogen flux for 10 min. Target molecules were eluted by 5 mL of EtOAc followed by 5 mL of ACN before concentration to 1 droplet under nitrogen flux and addition of 500 μL of ACN. Chloroacetanilides and Metalaxyl contain a single nitrogen atom contributing to ≈ 5% of the total mass. This challenges nitrogen isotope measurements compared to carbon measurements (≈ 60% of the total molecular mass), and required an additional concentration by solvent evaporation to reach sufficient nitrogen (m/z 28) signal on GC-IRMS. The absence

of SPE extraction effect on carbon/nitrogen isotope compositions is detailed in Part 3.1. and in section S-4 of the SI.

Pesticide quantification was performed by gas chromatography (GC, Trace 1300, Thermo Fisher Scientific) coupled to a mass spectrometer (MS, ISQ[™], Thermo Fisher Scientific). Pesticide degradation products (DP) were identified by GC-MS in fullscan mode (Acetochlor, Alachlor and Butachlor) and by Liquid-Chromatography-Mass-Spectrometry (LC-MS) in selected-ion monitoring mode (Atrazine, Metalaxyl, Acetochlor, Alachlor, S-Metolachlor and Butachlor). Mass spectrometry, GC and LC parameters are provided in section S-2 of the SI. Due to the lack of commercial standards for most DPs, the reported normalized DP peak areas correspond to DP peak area relative to Alachlor-d13 (LC-MS internal standard) (Tsipi et al., 2015).

2.4. Carbon and nitrogen stable isotope analysis of pesticides

The C and N isotope compositions of the pesticides were measured using a GC-C-IRMS system consisting of a TRACE[™] Ultra Gas Chromatograph (ThermoFisher Scientific) coupled via a GC IsoLink/Conflow IV interface to an isotope ratio mass spectrometer (DeltaV plus, ThermoFisher Scientific) (Alvarez-Zaldívar et al., 2018). GC and IRMS conditions are given in section S-3 of SI. The δ¹³C and δ¹⁵N values were calibrated using a three-point calibration against the V-PDB and Air standards, respectively, using international reference materials AIEA600, USGS40 and USGS41 (σ < 0.05‰). The carbon and nitrogen isotope ratios were reported in δ notation in parts per thousand [‰] according to (Eq. (1) and Eq. (2)):

$$\delta^{13}\text{C} = \left(\frac{\left(\frac{^{13}\text{C}}{^{12}\text{C}} \right)_{\text{sample}}}{\left(\frac{^{13}\text{C}}{^{12}\text{C}} \right)_{\text{VPDB}}} - 1 \right) \times 1000 \quad (1)$$

$$\delta^{15}\text{N} = \left(\frac{\left(\frac{^{15}\text{N}}{^{14}\text{N}} \right)_{\text{sample}}}{\left(\frac{^{15}\text{N}}{^{14}\text{N}} \right)_{\text{air}}} - 1 \right) \times 1000 \quad (2)$$

In-house BTEX and IAEA-600 caffeine standards were measured every 10 samples to control the quality of δ¹³C and δ¹⁵N measurements, respectively. An in-house pesticide mixture standard, consisting of the 6 studied pesticides with known isotope composition, was also measured at least every ten injections. Average long term reproducibility δ¹³C and δ¹⁵N values of pesticides did not significantly differ (Δδ¹³C_{EA-IRMS-GC-IRMS} ≤ 0.7‰, Δδ¹⁵N_{EA-IRMS-GC-IRMS} ≤ 0.5‰, Table S-4) from values obtained at our isotope facility using an elemental analyzer-isotopic ratio mass spectrometer (Flash EA IsoLink[™] CN IRMS, Thermo Fisher Scientific). The reported uncertainties, including both accuracy and reproducibility were based on long term measurements standard deviations (±σ, Table S-4 of the SI), which were systematically larger than the standard deviation (σ) calculated from triplicate sample measurements.

2.5. Carbon and nitrogen isotopic fractionation

Bulk isotopic fractionations (ε) were calculated using the linearized form for the Rayleigh equation (Eq. (3)).

$$\ln \left(\frac{\delta^{13}\text{C}_t + 1000}{\delta^{13}\text{C}_0 + 1000} \right) = \frac{\epsilon_C}{1000} \times \ln \left(\frac{C_t}{C_0} \right) \quad (3)$$

where δ¹³C₀ and δ¹³C_t are the measured carbon (or δ¹⁵N₀ and δ¹⁵N_t

for nitrogen) isotope ratios at the beginning ($t = 0$ day) and at t days from the beginning of the experiment, and C_0 and C_t are the corresponding concentrations. The error of isotopic fractionation ϵ is given as the 95% confidence interval (CI) and determined using regression analysis as described earlier (Elsner et al., 2007). In our experiment, C and N stable isotopic fractionation (i.e., ϵ_C and ϵ_N values) were not affected by temperature ($p > 0.05$) because they are primarily related to the cleavage mechanism and not to the process intensity (see SI, Table S6). Data obtained for experiments at 20 °C and 30 °C were thus combined to derive ϵ values.

The primary position-specific apparent kinetic isotope effects (AKIE) were calculated from the isotopic fractionation (ϵ) according to Eq. (4) (Elsner et al., 2005).

$$AKIE \approx \frac{1}{1 + z \times \left(\frac{n}{x}\right) \times \frac{\epsilon}{1000}} \quad (4)$$

where n is the number of atoms of a given element, x is the number of indistinguishable reactive positions, and z is the number of positions in intramolecular competition. Details of the parameters used for the six pesticides are given in section S-5 of SI. The uncertainty of AKIE values was estimated by error propagation calculations (Fischer et al., 2010).

2.6. C–N dual element isotope plots

The $\delta^{13}\text{C}$ and $\delta^{15}\text{N}$ values were plotted against each other to give the slopes of the regression lines (Λ , Eq. (5)) and to compare their isotope effects (Meyer et al., 2014):

$$\Lambda = \frac{\Delta\delta^{15}\text{N}}{\Delta\delta^{13}\text{C}} \sim \frac{\epsilon_{\text{average, nitrogen}}}{\epsilon_{\text{average, carbon}}} \quad (5)$$

In the dual element isotope plot, the slopes of the regression lines (Λ) are equal to $\epsilon_{\text{Nitrogen}}/\epsilon_{\text{Carbon}}$ and, therefore, reveal the footprint of underlying isotope effects (Elsner et al., 2005; Meyer et al., 2014).

2.7. Enantiomeric fractionation and C-ESIA

Metalaxyl is a chiral compound with the S-Metalaxyl and the R-Metalaxyl enantiomers. Change in the proportion of each enantiomer was calculated by $EF_{S\text{-Metalaxyl}}$ and $EF_{R\text{-Metalaxyl}}$ enantiomeric fractionation according to Eq. (6):

$$EF_{S\text{-Metalaxyl}} = \frac{\text{Peak area}_{S\text{-Metalaxyl}}}{\text{Peak area}_{S\text{-Metalaxyl}} + \text{Peak area}_{R\text{-Metalaxyl}}} \quad (6)$$

Racemic-Metalaxyl mixture then displays $EF_{S\text{-Metalaxyl}} = 0.5$, while an enriched S-Metalaxyl solution yields an $EF_{S\text{-Metalaxyl}} > 0.5$.

C-ESIA allows to determine the isotope composition of S-Metalaxyl and R-Metalaxyl enantiomers. Details of the GC and IRMS conditions for Metalaxyl C-ESIA are provided in (Masbou et al., 2018). Enantio-specific isotope parameters ($\delta^{13}\text{C}_{S\text{-Metalaxyl}}$, $\delta^{13}\text{C}_{R\text{-Metalaxyl}}$, $\epsilon_{S\text{-Metalaxyl}}$, $\epsilon_{R\text{-Metalaxyl}}$, $AKIE_C$ (S-Metalaxyl) and $AKIE_C$ (R-Metalaxyl)) were determined by similar calculations as for CSIA (Eq. (1) to (4), (Badea and Danet, 2015)).

2.8. Statistical analysis

Rate constants (k) (and associated half-life, i.e., DT_{50}) were determined using a Single First-Order Rate Model (SFO) from plots of $\ln(C/C_0)$ versus time (see section S-5 of SI). For slope comparison, Real Statistics Resource Pack for Microsoft Excel[®] provided by <http://www.real-statistics.com> was used. All data are displayed as

mean \pm σ .

3. Results and discussion

3.1. Validation of C–N dual-CSIA and C-ESIA methods

The developed C–N dual-CSIA and C-ESIA methods were suitable for the range of pH and DOC concentrations encountered in the hydrolysis experiment. The minimum peak amplitudes m/z 44 for linear $\delta^{13}\text{C}$ measurements were ≈ 300 mV for all the compounds, except for Butachlor (m/z 44 ≈ 500 mV, Table 2, Figure S-2), which corresponds to 5–8 ng of carbon injected on column. Linearity tests also revealed minimum m/z 28 amplitudes ranging from 150 to 200 mV (and 300 mV for Atrazine, Figure S-3), corresponding to 17–21 ng (37 ng for Atrazine) of nitrogen injected. For both nitrogen and carbon measurements, analytical error ($n = 3$) and long term reproducibility was $0.3\% \leq \sigma \leq 0.8\%$ (Table 2), which was consistent with previous studies (Meyer et al., 2008). No significant shift ($\Delta\delta^{13}\text{C} \leq 0.7\%$ and $\Delta\delta^{15}\text{N} \leq 0.5\%$) compare to EA-IRMS measurements confirmed the absence of significant carbon and nitrogen isotope fractionation during GC-IRMS analysis (Table 2). Method validation was also carried out for C-ESIA of Metalaxyl, using racemic-Metalaxyl and M-Metalaxyl (i.e. R enantiomer enriched formulation) standards (Masbou et al., 2018).

For the six pesticides, independently of pH and DOC concentrations, extraction recoveries were larger than 80%, except for Butachlor (recovery $\approx 60\%$). Hence, pH did not affect SPE extraction efficiency using C18 cartridges. Comparison with EA-IRMS measurements indicated limited effects of extraction methods using SPE on C and N isotope composition ($\Delta\delta^{13}\text{C} \leq 1\%$ and $\Delta\delta^{15}\text{N} \leq 0.5\%$, Table 2).

3.2. Hydrolysis of Atrazine and isotopic fractionation

Atrazine was hydrolysed under both acidic ($\text{pH} \leq 4$) and alkaline conditions ($\text{pH} = 12$), whereas it was not significantly degraded ($DT_{50} > 200$ days, $p > 0.05$), even with DOC addition and at circumneutral pH ($\text{pH} \approx 7$, Table S-8). At 20 °C, kinetic parameters decreased from $k = 0.009 \pm 0.002$ days⁻¹ at $\text{pH} = 4$ up to $k = 0.033 \pm 0.005$ days⁻¹ at $\text{pH} = 12$, with an intermediate $k = 0.013 \pm 0.001$ days⁻¹ at $\text{pH} = 2$, in agreement with previous observations (Meyer et al., 2008). As predicted by the Arrhenius equation, temperature affected kinetics parameters ($k_{20^\circ\text{C}}$ versus $k_{30^\circ\text{C}}$) with systematically faster kinetics at 30 °C ($p < 0.05$). Atrazine degradation kinetic at $\text{pH} = 2$ was 5 time faster at 30 °C compared to 20 °C, corresponding to an activation energy of 124 kJ mol⁻¹ (see section S-5 in SI for details). Similar activation energy of 95 kJ mol⁻¹ was found at $\text{pH} = 12$, which is consistent with 100 and 104 kJ mol⁻¹ in acidic and alkaline conditions (Grzybkowska et al., 2014). The systematic detection of hydroxy-2-Atrazine degradation product (See SI, Table S-2 and Figure S-11) indicates nucleophilic substitution of the chlorine atom by a hydroxyl group (Meyer et al., 2008).

An opposite $\epsilon_N = 1.3 \pm 0.6\%$ at $\text{pH} = 2$ and $\epsilon_N = -0.8 \pm 0.5\%$ at $\text{pH} = 12$ revealed different intermediate mechanisms leading to hydroxy-2-Atrazine in both cases (see Table S-9 for a comparison of results from this study with those of Meyer et al., 2008). Nitrogen inverse kinetic isotope effect under acidic conditions may result from an additional step of protonation at one of the N atom (Meyer et al., 2008). The ϵ_N values records a secondary kinetic isotope effects since all N atoms are embedded in the aromatic π -system that can be disrupted by reaction at the C–Cl position, implying an adjacent α -carbon (Figure S-11). As primary kinetic isotope effect recorders, carbon isotopic fractionation did not significantly vary (from $\epsilon_C = -6.1 \pm 0.8\%$ at $\text{pH} = 2$ to $\epsilon_C = -5.6 \pm 0.8\%$ at $\text{pH} = 12$).

Table 2
Validation of C–N CSIA methods. EA-IRMS, GC-C-IRMS $\delta^{13}\text{C}$ and $\delta^{15}\text{N}$ values (mean \pm σ , ‰) for pesticide standards are compared with GC-C-IRMS values for solid phase of extracted pesticide standards. Data are given for SPE extraction at pH = 7 (see Table S-5 in the SI for other pH values).

Compound	$\delta^{13}\text{C}$ (‰)		GC-IRMS Extracted (n = 3)	$\Delta\delta^{13}\text{C}$ (‰)		$\delta^{15}\text{N}$ (‰)		$\Delta\delta^{15}\text{N}$ (‰)		
	EA-IRMS (n = 3)	GC-IRMS (n)		EA-IRMS vs. GC-IRMS (‰)	EA-IRMS vs. Extracted (‰)	EA-IRMS (n = 3)	GC-IRMS (n)	GC-IRMS Extracted (n = 3)	EA-IRMS vs. GC-IRMS (‰)	EA-IRMS vs. Extracted (‰)
Atrazine	-26.3 ± 0.1	-26.3 ± 0.6 (n = 65)	-26.9 ± 0.2	0.1 ± 0.7	0.6 ± 0.3	-0.2 ± 0.1	-0.2 ± 0.4 (n = 30)	-0.1 ± 0.2	0.0 ± 0.5	-0.1 ± 0.3
Acetochlor	-29.3 ± 0.1	-29.6 ± 0.5 (n = 68)	-29.8 ± 0.1	0.3 ± 0.6	0.5 ± 0.2	-2.2 ± 0.1	-2.1 ± 0.6 (n = 23)	-1.7 ± 0.3	0.1 ± 0.7	-0.4 ± 0.7
Alachlor	-33.8 ± 0.1	-34.2 ± 0.4 (n = 55)	-34.5 ± 0.1	0.4 ± 0.5	0.7 ± 0.2	n.m	n.m	n.m	n.m	n.m
Butachlor	-26.8 ± 0.1	-27.5 ± 0.5 (n = 58)	-27.3 ± 0.1	0.7 ± 0.6	0.5 ± 0.2	1.1 ± 0.1	1.0 ± 0.7 (n = 39)	1.0 ± 0.2	0.2 ± 0.8	0.1 ± 0.2
S-Metolachlor	-30.9 ± 0.1	-31.2 ± 0.5 (n = 74)	-31.4 ± 0.1	0.3 ± 0.6	0.5 ± 0.2	0.4 ± 0.1	0.4 ± 0.7 (n = 34)	0.3 ± 0.1	0.1 ± 0.7	0.2 ± 0.2
Metalaxyl	-31.7 ± 0.1	-31.8 ± 0.8 (n = 47)	-31.7 ± 0.1	0.1 ± 0.9	0.1 ± 0.2	0.4 ± 0.1	0.8 ± 0.3 (n = 26)	0.6 ± 0.3	0.5 ± 0.4	-0.2 ± 0.4

n.m: not measured.

These results confirm that C–N dual element isotope plots allow distinguishing oxidative dealkylation from biotic/abiotic hydrolysis of Atrazine (Meyer et al., 2008). The same approach can be applied to examine underlying isotope effects during hydrolysis of anilide pesticides.

3.3. Hydrolysis of chloroacetanilides and isotopic fractionation

Hydrolysis of chloroacetanilides was only observed under alkaline conditions (pH = 12) and DOC addition did not influence hydrolysis at pH = 7 (Table S8). All chloroacetanilide molecules underwent hydrolysis at 30 °C with similar degradation kinetics ($k = 0.038 \pm 0.003 \text{ days}^{-1}$ for Acetochlor, $k = 0.038 \pm 0.004 \text{ days}^{-1}$ for Alachlor, $k = 0.027 \pm 0.005 \text{ days}^{-1}$ for Butachlor), with the exception of S-Metolachlor ($k = 0.006 \pm 0.001 \text{ days}^{-1}$ at 30 °C and insignificant hydrolysis at 20 °C). Hydrolysis kinetics for Acetochlor, Alachlor and Butachlor in experiment at 30 °C were 3–4 fold faster compared to those in experiments at 20 °C. This corresponds to activation energies ranging from 70 to 100 kJ mol^{-1} (see section S-5 of the SI for details). Except for S-Metolachlor, for which no degradation products was identified, mass spectra interpretation and comparison with literature (Zheng and Ye, 2001) indicates the formation of N-(2,6-diethylphenyl)-2-hydroxy-N-(methoxymethyl)acetamide, N-(ethoxymethyl)-N-(2-ethyl-6-methylphenyl)-2-hydroxyacetamide and N-(2,6-diethylphenyl)-2-hydroxy-N-(butoxymethyl)acetamide as degradation products for Alachlor, Acetochlor and Butachlor hydrolysis, respectively (see Table S-2 for

chemical structures). Inspection of mass spectra obtained by both GC-MS and LC-MS running in full-scan mode did not allow to detect other degradation products (Figure S-1). The occurrence of hydroxylated degradation products in all experiments revealed nucleophilic substitution at the C–Cl bond position of the chloroacetanilide pesticides (see Fig. 3 for Alachlor, and Figure S-8 and Figure S-9 in the SI for Acetochlor and Butachlor, respectively). Our results are consistent with those obtained during alkaline (NaOH 2 N) hydrolysis of chloroacetanilides (Carlson et al., 2006). In few cases, however, an additional pathway involving amide cleavage was observed, that we could not exclude for S-Metolachlor under alkaline hydrolysis as no degradation products were unequivocally identified.

Acetochlor, Alachlor and Butachlor displayed similar carbon isotopic fractionation during abiotic hydrolysis ($\epsilon_{\text{C}} = -4.0 \pm 0.8\%$, $\epsilon_{\text{C}} = -4.9 \pm 0.4\%$ and $\epsilon_{\text{C}} = -3.7 \pm 0.7\%$, respectively), whereas ϵ_{C} for S-Metolachlor was lower ($-2.8 \pm 0.6\%$, Table 3). In comparison, ϵ_{C} values have been obtained for biotic degradation of S-Metolachlor ($\epsilon_{\text{C}} \approx 0\%$, degradation $\leq 30\%$), Alachlor ($\epsilon_{\text{C}} = -2.0 \pm 0.3\%$, degradation $\leq 60\%$) and Acetochlor ($\epsilon_{\text{C}} = -3.4 \pm 0.5\%$, degradation $\leq 65\%$) in a constructed wetland (Elsayed et al., 2014) or for S-Metolachlor biotic degradation ($\epsilon_{\text{C}} = -1.5 \pm 0.5\%$, degradation $\geq 80\%$) in soil incubation experiments (Alvarez-Zaldívar et al., 2018). Small differences in isotopic fractionation during chloroacetanilide hydrolysis and biotic degradation may reflect distinct mechanisms, which is supported by the formation of different degradation products. For instance, oxanilic (OXA) and

Table 3
Bulk (C–N CSIA) and enantiospecific (C-ESIA) isotopic fractionation (ϵ_{C} and ϵ_{N}) for the studied pesticides during acidic or alkaline hydrolysis. Apparent Kinetic Isotope Effects (AKIE_C and AKIE_N) and Λ values were calculated using Eqs. (4) and (5), respectively. Uncertainties are given as 95% CI.

		Hydrolysis type	ϵ_{C} (‰)	ϵ_{N} (‰)	$\Lambda = \delta^{13}\text{C}/\delta^{15}\text{N} = \epsilon_{\text{C}}/\epsilon_{\text{N}}$	AKIE _C	AKIE _N
C–N CSIA	Atrazine	Acidic	-6.1 ± 0.8	1.3 ± 0.6	-0.29 ± 0.12	1.052 ± 0.006	0.994 ± 0.001
	Atrazine	Alkaline	-5.6 ± 0.8	-0.8 ± 0.5	0.15 ± 0.08	1.047 ± 0.006	1.001 ± 0.001
	Acetochlor	Alkaline	-4.0 ± 0.8	n.s	n.s	1.060 ± 0.012	n.s
	Alachlor	Alkaline	-4.9 ± 0.4	n.m	n.m	1.073 ± 0.005	n.m
	Butachlor	Alkaline	-3.7 ± 0.7	n.s	n.s	1.067 ± 0.013	n.s
	S-Metolachlor	Alkaline	-2.8 ± 0.6	-2.0 ± 1.3	0.79 ± 0.71	1.043 ± 0.008	1.002 ± 0.001
	M-Metalaxyl	Alkaline	-2.1 ± 1.1	-2.2 ± 0.2	1.05 ± 0.51	1.033 ± 0.017	1.002 ± 0.001
	Rac-Metalaxyl	Alkaline	-3.0 ± 0.4	-2.7 ± 0.7	0.86 ± 0.46	1.047 ± 0.007	1.003 ± 0.001
C-ESIA	S-Metalaxyl	Alkaline	-2.8 ± 1.2	n.m	n.m	1.044 ± 0.018	n.m
	R-Metalaxyl		-2.5 ± 0.8	n.m	n.m	1.040 ± 0.012	n.m

n.s: not significant.

n.m: not measured.

ethanesulfonic acids (MESA) prevailed in wetlands (Maillard et al., 2016) but were not detected in this study.

Weak nitrogen isotopic fractionation ($\Delta\delta^{15}\text{N} \approx 1.5\text{‰}$) for Alachlor, Acetochlor and Butachlor did not allow to derive ϵ_{N} values given the analytical precision ($\approx 1\text{‰}$). In contrast, S-Metolachlor displayed small but significant $\epsilon_{\text{N}} = -2.0 \pm 1.3\text{‰}$. Since S-Metolachlor contains a single nitrogen heteroatom, nitrogen isotope effect is position specific and secondary. The absence of isotope dilution effect likely resulted in larger ϵ_{N} values for S-Metolachlor compared to Atrazine ($\epsilon_{\text{N}} = -0.8 \pm 0.5\text{‰}$). However, $\text{AKIE}_{\text{N}} = 1.002 \pm 0.001$ for S-Metolachlor was, as expected, similar to $\text{AKIE}_{\text{N}} = 1.001 \pm 0.001$ for Atrazine.

3.4. Hydrolysis of chiral metalaxyl and C–N isotopic fractionation

Independent hydrolysis experiments with racemic-Metalaxyl and R enantiomer enriched (M-Metalaxyl) formulations were conducted to evaluate enantiomeric and isotopic fractionation of Metalaxyl formulations with different proportions of active stereoisomers.

Racemic-Metalaxyl degraded at $\text{pH} = 9$ and 30°C ($k = 0.010 \pm 0.002 \text{ days}^{-1}$). Degradation kinetic was particularly high at $\text{pH} = 12$ ($k = 0.29 \pm 0.02 \text{ h}^{-1}$), in agreement with previous observations (Sharom and Edgington, 1982). Enantiomeric fractionation could not be observed during abiotic degradation, and enantiomeric ratios ($\text{EF} \approx 0.5$) did not change significantly across the experiment (Fig. 1), which is consistent with previous studies (Maia et al., 2017). Identical degradation kinetics ($k = 0.29 \pm 0.02 \text{ h}^{-1}$) for degradation of M-Metalaxyl further confirmed this assumption.

Demethyl-metalaxyl acid was the main degradation products detected during Metalaxyl hydrolysis, while hydroxylated compounds could not be detected (Fig. 1). Ester cleavage via $\text{S}_{\text{N}}2$ type dealkylation is a common transformation pathway for organic molecules (Mc Murry, 1976) and may be favoured by the absence of chlorine atom in the Metalaxyl molecule. In soils, Metalaxyl was degraded by both dealkylation (Sukul and Spitteller, 2000) and hydroxylation (Masbou et al., 2018).

Racemic-Metalaxyl and M-Metalaxyl hydrolysis yielded similar carbon isotopic fractionation ($\epsilon_{\text{C}} = -3.0 \pm 0.4\text{‰}$ and $\epsilon_{\text{C}} = -2.1 \pm 1.1\text{‰}$, respectively), suggesting a similar fractionation pattern among enantiomers. Similar ϵ_{C} values for S-Metalaxyl ($\epsilon_{\text{C}} = -2.8 \pm 1.2\text{‰}$) and R-Metalaxyl ($\epsilon_{\text{C}} = -2.5 \pm 0.8\text{‰}$) obtained by carbon enantiospecific stable isotope analysis (C-ESIA) during

racemic-Metalaxyl degradation indicated the absence of enantioselective isotopic fractionation during alkaline hydrolysis.

Worthy of note, ϵ_{C} values for hydrolysis were close to those for racemic-Metalaxyl in soil degradation experiment ($\epsilon_{\text{C}} = -0.9 \pm 0.5\text{‰}$ and $\epsilon_{\text{C}} = -2.0 \pm 1.3\text{‰}$ in vineyard and crop soils respectively (Masbou et al., 2018)). As for carbon, nitrogen isotopic fractionations for hydrolysis were similar for racemic-Metalaxyl ($\epsilon_{\text{N}} = -2.7 \pm 0.7\text{‰}$) and M-Metalaxyl ($\epsilon_{\text{N}} = -2.2 \pm 0.2\text{‰}$). However, ϵ_{N} values slightly differed from those obtained in soil biodegradation experiment where hydroxylation was observed ($\epsilon_{\text{N}} = -1.2 \pm 0.9\text{‰}$ in the vineyard soil; see section S-9 of the SI). Altogether, the results suggest that C–N dual-CSIA bears potential to tease apart Metalaxyl dealkylation from hydroxylation in the field.

3.5. AKIEs dependence from bond cleavage: insights from C–N isotope plots

AKIE_{C} values derived from isotopic fractionation for both alkaline and acidic hydrolysis (Table 3) ranged from 1.033 to 1.073 for all the pesticides, which is consistent with primary isotope effect during $\text{S}_{\text{N}}2$ type mechanisms ($\text{AKIE}_{\text{C}} = 1.03\text{--}1.07$ (Elsner et al., 2005)). Small differences occurred between AKIE_{C} values for C–Cl bond cleavage (AKIE_{C} ranged from 1.047 to 1.073 for Atrazine, Alachlor, Acetochlor, and Butachlor), and those observed for other bond cleavage (AKIE_{C} values ranged from 1.033 to 1.047 for Metalaxyl (C–O cleavage) and S-Metolachlor (undetermined reaction). Despite the occurrence of primary isotope effects and AKIE_{C} calculation that limit isotopic dilution effects, carbon isotopic fractionations lack of sensitivity to tease apart hydrolysis mechanisms. As anilide pesticides contain 1–3 N heteroatoms, dual C–N isotope analysis may circumvent the issue of isotope effect ‘dilution’ encountered with C isotopes and show sufficient sensitivity to distinguish hydrolysis mechanisms.

Secondary nitrogen isotope effect occurred for all molecules, except for S-Metolachlor. Despite low AKIE_{N} values ranging from 0.994 to 1.003, dual plot of $\delta^{13}\text{C}$ versus $\delta^{15}\text{N}$ values suggests that degradation mechanism for Acetochlor and Butachlor during hydrolysis differ from that of Metalaxyl and S-Metolachlor (Fig. 2). Although Acetochlor and Butachlor did not display significant nitrogen isotopic fractionation ($\leq 1.5\text{‰}$), C–N isotope fractionation patterns for Metalaxyl and S-Metolachlor ($\Delta = 0.86 \pm 0.46$ and $\Delta = 0.79 \pm 0.71$, respectively) appear similar. Isotopic fractionation patterns in dual plots thus revealed the footprint of underlying

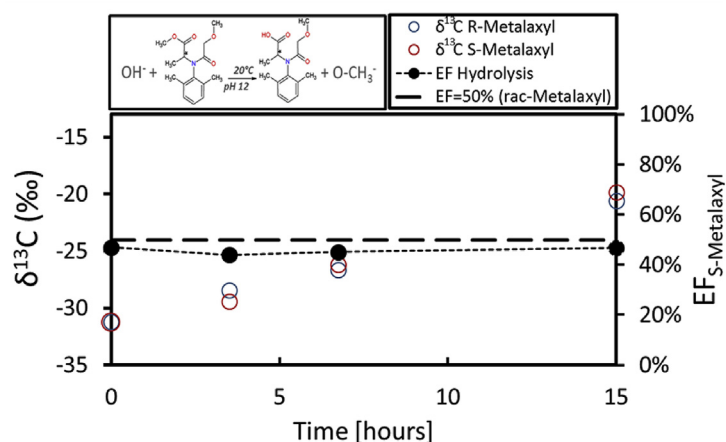


Fig. 1. $\delta^{13}\text{C}_{\text{S-Metalaxyl}}$ (‰, left axis), $\delta^{13}\text{C}_{\text{R-Metalaxyl}}$ (‰, left axis), and $\text{EF}_{\text{S-Metalaxyl}}$ (% , right axis) values during hydrolysis ($\text{pH} = 12$, 20°C). Error bars correspond to the total analytical uncertainty ($\pm\sigma$), which incorporates both accuracy and reproducibility of long term measurements (see Table S-4 in the SI), and can be smaller than the symbols.

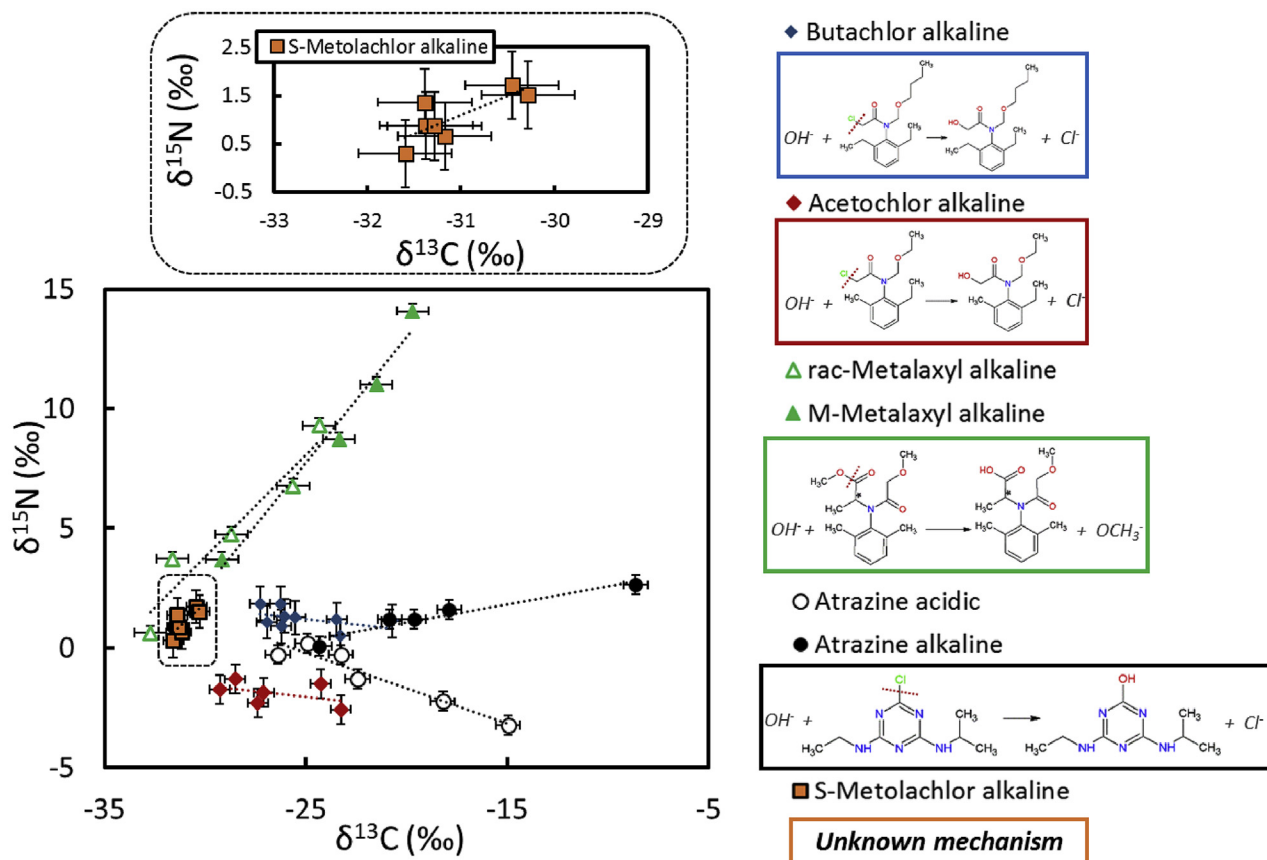


Fig. 2. C-N isotope plot for carbon and nitrogen for Atrazine, Metalaxyl (racemic and R enantiomer formulation (M-Metalaxyl)) and S-Metolachlor during acidic and/or alkaline hydrolysis. S-Metolachlor data are zoomed at the top of the figure. Error bars correspond to the total analytical uncertainty ($\pm \sigma$), which incorporates both accuracy and reproducibility of long term measurements (see Table S-4 in the SI), and can be smaller than the symbols. Displayed linear regression are significant except for Butachlor and Acetochlor ($p > 0.05$).

isotope effects for (i) Acetochlor, Alachlor and Butachlor, which undergo S_N2 C-Cl bond breaking in alkyl chain, (ii) Atrazine undergoing S_N2 C-Cl bond breaking in the aromatic π -system, and (iii) Metalaxyl, which likely undergo S_N2 C-O bond breaking. Further work is needed to minimize analytical uncertainties and enhance interpretation when degradation extent and/or isotope fractionation are modest.

3.6. $\delta^{13}\text{C}$ values of hydrolysis degradation products

Pesticide degradation products (DP) may be more polar than their parent compounds (PC), thereby limiting their measurement using GC-IRMS. GC-IRMS detection of Acetochlor, Alachlor and Butachlor DP formed during alkaline hydrolysis allowed to follow the isotopic composition of DP versus PC during hydrolysis in the closed laboratory experiments. In addition to DP/PC ratios, carbon isotope ratios of chloroacetanilides and DP may be used to evaluate degradation state of chloroacetanilides and their DP under field conditions.

DP formed during alkaline hydrolysis were isotopically lighter than their corresponding parent compounds. For instance, $\delta^{13}\text{C}$ values of Alachlor increased from $-34.3 \pm 0.1\text{‰}$ to $-32.3 \pm 0.1\text{‰}$, while corresponding degradate got progressively lighter from $-33.9 \pm 0.3\text{‰}$ to $-37.4 \pm 0.4\text{‰}$ in experiments at 20°C (Fig. 3). However, the effect of extraction procedure on recovery and isotopic fractionation could not be evaluated because commercially available standards for the detected DP are currently lacking. Nevertheless, a mass balance ($[\text{DP} + \text{PC}]_t = [\text{PC}]_0$) and isotope

balance ($\delta^{13}\text{C}_{\text{DP+PC,t}} = \delta^{13}\text{C}_{\text{PC,0}}$) were established based on CO_2 peak areas integration (GC-IRMS) and assuming the formation of a unique DP for Alachlor, Acetochlor and Butachlor and no isotopic effects for DP extraction and analysis (see section S-7 in SI for details). Mass balance ($[\text{DP} + \text{PC}]_t / [\text{PC}]_0 \geq 90\%$, Table S-11) and isotope balance ($\delta^{13}\text{C}_{\text{DP+PC,t}} / \delta^{13}\text{C}_{\text{PC,0}} \geq 90\%$, Table S-11) for experiments at 20°C support the notion that a unique DP was formed and acquired the complement isotope signature of its PC.

A similar pattern was observed in experiments at 30°C , although amount of DP and $\delta^{13}\text{C}$ values did not change until $t = 9$ days (Fig. 3). While a single DP likely occurred until $t = 9$ days ($\delta^{13}\text{C}_{\text{DP+PC,t}} / \delta^{13}\text{C}_{\text{PC,0}} \geq 90\%$, Table S-11), mass balance estimations further suggest degradation of DP after 30 days ($\delta^{13}\text{C}_{\text{DP+PC,t}} / \delta^{13}\text{C}_{\text{PC,0}} \approx 70\%$, Table S-11 in the SI). Small changes in the $\delta^{13}\text{C}$ values of the degradation product (Fig. 3) likely reflect a balance between DP formation in the experiments at 30°C , with concomitant enrichment in ^{12}C , and DP degradation, leading to an enrichment in ^{13}C . However, no degradates from the initially formed DP were detected by GC-MS or LC-MS analysis. This may be due to low SPE extraction recoveries with C-18 cartridges that mainly target nonpolar to moderately polar compounds.

Altogether, when a unique and stable degradation product is ideally formed, values of $\delta^{13}\text{C}_{\text{PC,t}}$ and $\delta^{13}\text{C}_{\text{PC,t}}$ obtained from the same water sample may be a proxy of the initial isotope ratio $\delta^{13}\text{C}_{\text{PC,0}}$. This can help to determine in some cases the $\delta^{13}\text{C}_{\text{PC,0}}$ source signature, often encountered when evaluating pesticide degradation in the field.

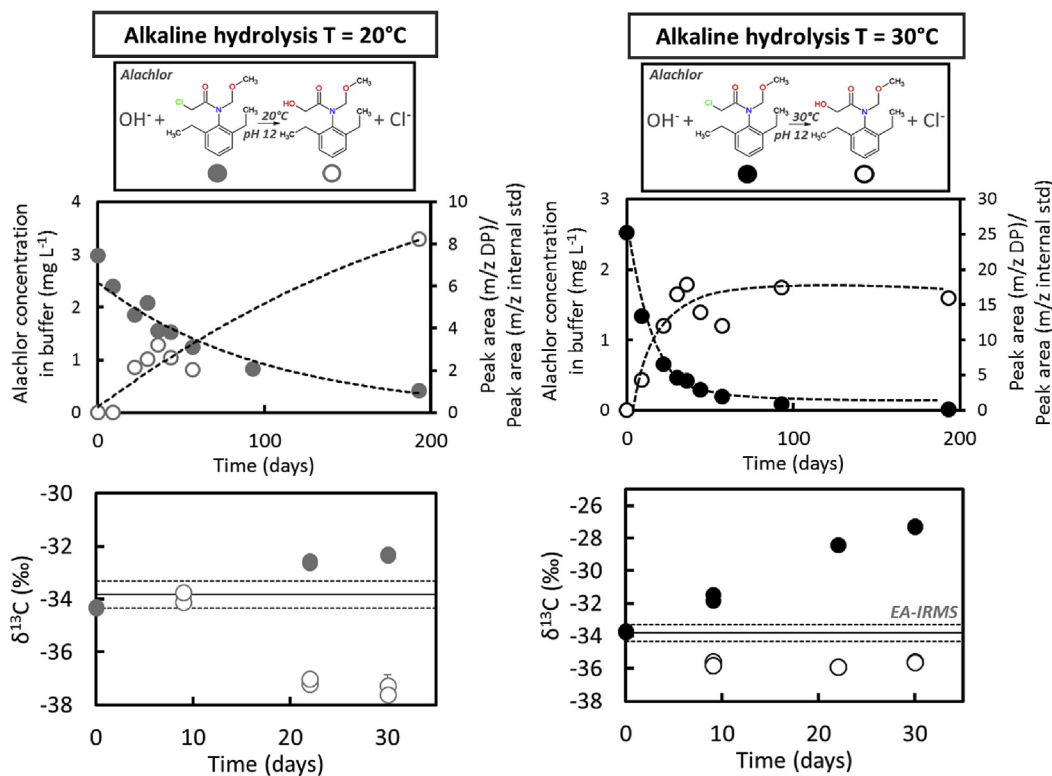


Fig. 3. Alachlor concentrations (filled symbols) and alachlor degradation products (DP, open symbols) peak areas normalized with internal standard peak areas (top), and corresponding $\delta^{13}\text{C}$ values (down) during alkaline hydrolysis (pH = 12) at 20 °C (left) and 30 °C (right). Error bars correspond to the total analytical uncertainty ($\pm\sigma$), which incorporates both accuracy and reproducibility of long term measurements (see Table S-4 in the SI), and can be smaller than the symbols.

4. Conclusions

Abiotic hydrolysis of Acetochlor, Alachlor, S-Metolachlor, Butachlor, Metalaxyl, and Atrazine at most common environmental pH ($4 < \text{pH} < 9$) is a slow process ($\text{DT}_{50} > 200$ days) associated with insignificant isotopic fractionation ($\Delta\delta^{13}\text{C} \leq 0.5\text{‰}$). Abiotic hydrolysis of studied pesticides thus may be neglected in most CSIA studies when pH of surface and groundwater systems ranges between 6 and 8.5, although hydrolysis may also occur locally at water-mineral interface in aquifer (Smolen and Stone, 1997). Only Metalaxyl was significantly degraded during hydrolysis at pH = 9, which resulted in significant isotopic fractionation ($\epsilon_{\text{C}} = -4.2 \pm 1.5\text{‰}$). In contrast, significant hydrolysis occurred at pH < 4 and pH > 9. Pesticide degradation ranged from a few hours (Metalaxyl, pH = 12) to several weeks (S-Metalaxyl, pH = 12) under alkaline conditions, which may occur in carbonate-rich minerals drainage (pH \approx 10–12, (Khouri et al., 1992; Möller and Bau, 1993)). Most importantly, the combination of degradation products analysis and C–N dual-CSIA allowed to elucidate degradation mechanisms of chloroacetanilide and acylalanine pesticides. These first reference isotopic fractionation values for hydrolysis of anilide pesticides can be compared in the future with ^{15}N and ^{13}C fractionation patterns during microbial degradation, and used to tease apart degradation pathways in the field.

Acknowledgements

Jeremy Masbou was supported by a fellowship of the EU-INTERREG V upper Rhine project 1.6 SERIOR (Security Risk Orientation). The authors wish to acknowledge Benoît Guyot for support in sampling, analyses of DP and fruitful discussions. Maurice Millet

is acknowledge for his help with LC-MS measurements.

Appendix A. Supplementary data

Supplementary data related to this article can be found at <https://doi.org/10.1016/j.chemosphere.2018.09.056>.

References

- Alvarez-Zaldívar, P., Payraudeau, S., Meite, F., Masbou, J., Imfeld, G., 2018. Pesticide degradation and export losses at the catchment scale: in sights from compound-specific isotope analysis (CSIA). *Water Res.* 139, 198–207.
- Armanpour, S., Bing, L., 2015. Adsorption of herbicide butachlor in cultivated soils of golestan province, Iran. *J. Geosci. Environ. Protect.* 3, 15.
- Atwood, D., Paisley-Jones, C., 2017. Pesticides Industry Sales and Usage 2008–2012 Market Estimates. US Environmental Protection Agency, Washington, DC (Google Scholar).
- Badea, S.-L., Danet, A.-F., 2015. Enantioselective stable isotope analysis (ESIA) — a new concept to evaluate the environmental fate of chiral organic contaminants. *Sci. Total Environ.* 514, 459–466.
- Carlson, D.L., Than, K.D., Roberts, A.L., 2006. Acid- and base-catalyzed hydrolysis of chloroacetamide herbicides. *J. Agric. Food Chem.* 54, 4740–4750.
- Elsayed, O., Maillard, E., Vuilleumier, S., Nijenhuis, I., Richnow, H., Imfeld, G., 2014. Using compound-specific isotope analysis to assess the degradation of chloroacetanilide herbicides in lab-scale wetlands. *Chemosphere* 99, 89–95.
- Elsner, M., 2010. Stable isotope fractionation to investigate natural transformation mechanisms of organic contaminants: principles, prospects and limitations. *J. Environ. Monit.* 12, 2005–2031.
- Elsner, M., Imfeld, G., 2016. Compound-specific isotope analysis (CSIA) of micro-pollutants in the environment — current developments and future challenges. *Curr. Opin. Biotechnol.* 41, 60–72.
- Elsner, M., McKelvie, J., Lacrampe Couloume, G., Sherwood Lollar, B., 2007. Insight into methyl tert-butyl ether (MTBE) stable isotope fractionation from abiotic reference experiments. *Environ. Sci. Technol.* 41, 5693–5700.
- Elsner, M., Zwank, L., Hunkeler, D., Schwarzenbach, R.P., 2005. A new concept linking observable stable isotope fractionation to transformation pathways of organic pollutants. *Environ. Sci. Technol.* 39, 6896–6916.
- Fenner, K., Canonica, S., Wackett, L.P., Elsner, M., 2013. Evaluating pesticide degradation in the environment: blind spots and emerging opportunities. *Science*

- 341, 752–758.
- Fischer, A., Weber, S., Reineke, A.-K., Hollender, J., Richnow, H.-H., 2010. Carbon and hydrogen isotope fractionation during anaerobic quinoline degradation. *Chemosphere* 81, 400–407.
- Grzybkowska, A., Kaminski, R., Dybala-Defratyka, A., 2014. Theoretical predictions of isotope effects versus their experimental values for an example of uncatalyzed hydrolysis of atrazine. *Phys. Chem. Chem. Phys.* 16, 15164–15172.
- Hartenbach, A.E., Hofstetter, T.B., Tentscher, P.R., Canonica, S., Berg, M., Schwarzenbach, R.P., 2008. Carbon, hydrogen, and nitrogen isotope fractionation during light-induced transformations of atrazine. *Environ. Sci. Technol.* 42, 7751–7756.
- Hoefs, J., 1997. *Stable Isotope Geochemistry*.
- Imfeld, G., Kopinke, F.-D., Fischer, A., Richnow, H.-H., 2014. Carbon and hydrogen isotope fractionation of benzene and toluene during hydrophobic sorption in multistep batch experiments. *Chemosphere* 107, 454–461.
- Khoury, H.N., Salameh, E., Clark, I.D., Fritz, P., Bajjali, W., Milodowski, A.E., Cave, M.R., Alexander, W.R., 1992. A natural analogue of high pH cement pore waters from the Maqarin area of northern Jordan. I: introduction to the site. *J. Geochem. Explor.* 46, 117–132.
- Komárek, M., Čadková, E., Chrástný, V., Bordas, F., Bollinger, J.-C., 2010. Contamination of vineyard soils with fungicides: a review of environmental and toxicological aspects. *Environ. Int.* 36, 138–151.
- Larson, R.A., Weber, E.J., 1994. *Reaction Mechanisms in Environmental Organic Chemistry*. CRC press.
- Lewis, K.A., Tziliavakis, J., Warner, D.J., Green, A., 2016. An international database for pesticide risk assessments and management. *Hum. Ecol. Risk Assess.* 22, 1050–1064.
- Lutz, S.R., van der Velde, Y., Elsayed, O.F., Imfeld, G., Lefrancq, M., Payraudeau, S., van Breukelen, B.M., 2017. Pesticide fate on catchment scale: conceptual modelling of stream CSIA data. *Hydrol. Earth Syst. Sci.* 21, 5243.
- Mabey, W., Mill, T., 1978. Critical review of hydrolysis of organic compounds in water under environmental conditions. *J. Phys. Chem. Ref. Data* 7, 383–415.
- Maia, A.S., Ribeiro, A.R., Castro, P.M., Tiritan, M.E., 2017. Chiral analysis of pesticides and drugs of environmental concern: biodegradation and enantiomeric fraction. *Symmetry* 9, 196.
- Maillard, E., Lange, J., Schreiber, S., Dollinger, J., Herbstritt, B., Millet, M., Imfeld, G., 2016. Dissipation of hydrological tracers and the herbicide S-metolachlor in batch and continuous-flow wetlands. *Chemosphere* 144, 2489–2496.
- Mandelbaum, R.T., Wackett, L.P., Allan, D.L., 1993. Rapid hydrolysis of atrazine to hydroxyatrazine by soil bacteria. *Environ. Sci. Technol.* 27, 1943–1946.
- Masbou, J., Meite, F., Guyot, B., Imfeld, G., 2018. Enantiomer-specific stable carbon isotope analysis (ESIA) to evaluate degradation of the chiral fungicide Metalaxyl in soils. *J. Hazard Mater.* 353, 99–107.
- Mazzuoli, S., Loisel, S., Hull, V., Bracchini, L., Rossi, C., 2003. The analysis of the seasonal, spatial, and compositional distribution of humic substances in a subtropical shallow lake. *Clean. - Soil, Air, Water* 31, 461–468.
- Mc Murry, J., 1976. Ester Cleavages via SN2-Type Dealkylation. *Organic Reactions*.
- Meyer, A.H., Dybala-Defratyka, A., Alaimo, P.J., Geronimo, I., Sanchez, A.D., Cramer, C.J., Elsner, M., 2014. Cytochrome P450-catalyzed dealkylation of atrazine by *Rhodococcus* sp. strain NI86/21 involves hydrogen atom transfer rather than single electron transfer. *Dalton Trans.* 43, 12175–12186.
- Meyer, A.H., Penning, H., Elsner, M., 2009. C and N isotope fractionation suggests similar mechanisms of microbial atrazine transformation despite involvement of different enzymes (AtzA and TrzN). *Environ. Sci. Technol.* 43, 8079–8085.
- Meyer, A.H., Penning, H., Lowag, H., Elsner, M., 2008. Precise and accurate compound specific carbon and nitrogen isotope analysis of atrazine: critical role of combustion oven conditions. *Environ. Sci. Technol.* 42, 7757–7763.
- Möller, P., Bau, M., 1993. Rare-earth patterns with positive cerium anomaly in alkaline waters from Lake Van, Turkey. *Earth Planet. Sci. Lett.* 117, 671–676.
- OECD, 2004. OECD Guidelines for the Testing of Chemicals-Hydrolysis as a Function of PH, vol. 111. OECD publishing OECD Test n°, p. 16.
- Schüth, C., Taubald, H., Bolaño, N., Maciejczyk, K., 2003. Carbon and hydrogen isotope effects during sorption of organic contaminants on carbonaceous materials. *J. Contam. Hydrol.* 64, 269–281.
- Sharom, M., Edgington, L., 1982. The adsorption, mobility, and persistence of metalaxyl in soil and aqueous systems. *J. Indian Dent. Assoc.* 4, 334–340.
- Smolen, J.M., Stone, A.T., 1997. Divalent metal ion-catalyzed hydrolysis of phosphorothionate ester pesticides and their corresponding oxonates. *Environ. Sci. Technol.* 31, 1664–1673.
- Sukul, P., Spiteller, M., 2000. Metalaxyl: persistence, degradation, metabolism, and analytical methods. *Rev. Environ. Contam. Toxicol.* 164, 1–26.
- Tsipi, D., Botitsi, H., Economou, A., 2015. *Mass Spectrometry for the Analysis of Pesticide Residues and Their Metabolites*. John Wiley & Sons.
- Wang, Y., Huang, Y., 2003. Hydrogen isotopic fractionation of petroleum hydrocarbons during vaporization: implications for assessing artificial and natural remediation of petroleum contamination. *Appl. Geochem.* 18, 1641–1651.
- Wu, L., Kümmel, S., Richnow, H.H., 2017. Validation of GC–IRMS techniques for $\delta^{13}\text{C}$ and $\delta^2\text{H}$ CSIA of organophosphorus compounds and their potential for studying the mode of hydrolysis in the environment. *Anal. Bioanal. Chem.* 409, 2581–2590.
- Zhang, N., Bashir, S., Qin, J., Schindelka, J., Fischer, A., Nijenhuis, I., Herrmann, H., Wick, L.Y., Richnow, H.H., 2014. Compound specific stable isotope analysis (CSIA) to characterize transformation mechanisms of α -hexachlorocyclohexane. *J. Hazard Mater.* 280, 750–757.
- Zheng, H.-H., Ye, C.-M., 2001. Identification of UV photoproducts and hydrolysis products of butachlor by mass spectrometry. *Environ. Sci. Technol.* 35, 2889–2895.